Developmental Biology 228, 73–85 (2000)


# Ectodermally Derived FGF8 Defines the Maxillomandibular Region in the Early Chick Embryo: Epithelial–Mesenchymal Interactions in the Specification of the Craniofacial Ectomesenchyme

**Yasuyo Shigetani, Yoshiaki Nobusada, and Shigeru Kuratani**[1]

*Department of Biology, Okayama University Faculty of Science, 3-1-1 Tsushimanaka, Okayama 700-8530, Japan*

**The most rostral cephalic crest cells in the chick embryo first populate ubiquitously in the rostroventral head. Before the influx of crest cells, the ventral head ectoderm expresses *Fgf8* in two domains that correspond to the future mandibular arch. *Bmp4* is expressed rostral and caudal to these domains. The rostral part of the *Bmp4* domain develops into the rostral end of the maxillary process that corresponds to the transition between the maxillomandibular and premandibular regions. Thus, the distribution patterns of FGF8 and BMP4 appear to foreshadow the maxillomandibular region in the head ectoderm. In the ectomesenchyme of the pharyngula embryo, expression patterns of some homeobox genes overlap the distribution of their upstream growth factors. *Dlx1* and *Barx1*, the targets of FGF8, are expressed in the mandibular ectomesenchyme, and *Msx1*, the target of BMP4, in its distal regions. Ectopic applications of FGF8 lead to shifted expression of the target genes as well as repatterning of the craniofacial primordia and of the trigeminal nerve branches. Focal injection of a lipophilic dye, DiI, showed that this shift was at least in part due to the posterior transformation of the original premandibular ectomesenchyme into the mandible, caused by the changed distribution of FGF8 that defines the mandibular region. We conclude that FGF8 in the early ectoderm defines the maxillomandibular region of the prepharyngula embryo, through epithelial–mesenchymal interactions and subsequent upregulation of homeobox genes in the local mesenchyme. BMP4 in the ventral ectoderm appears to limit the anterior expression of *Fgf8*. Ectopic application of BMP4 consistently diminished part of the mandibular arch.** © 2000 Academic Press

***Key Words:*** **ectomesenchyme; growth factors; homeobox genes; mandibular arch; chick embryo; neural crest.**

## INTRODUCTION

Cephalic neural crest cells give rise to the head ectomesenchyme, the fate of which is determined in part by intrinsic genetic programs involving, for example, expression of *Hox* genes in migrating crest cells, and in part by epithelial–mesenchymal interactions involving cell–cell signaling pathways including SHH, BMPs, and FGFs. A number of transcription factors, such as *Msx1* and *2*, *Dlx* genes, and *Barx1* (Tucker *et al.*, 1998a; Bei and Maas, 1998; Barlow *et al.*, 1999; Thomas *et al.*, 2000), appear to act downstream of BMPs and FGFs to exert patterning of neural-crest-derived structures in the head. These include the bones of the skull and the tooth and the skeletal system in the mandibular arch (Thesleff *et al.*, 1995; Bei and Maas, 1998; Barlow *et al.*, 1999). Expression of these genes is largely limited to the ectomesenchyme of the pharyngeal arches. These genes are known to function in the local specification of the mandibular arch (Tucker *et al.*, 1999a; Ferguson *et al.*, 2000). They are not expressed in the more rostral head mesenchyme. Located between the eye and the maxillary process, this crest-derived ectomesenchyme has not been studied extensively. These cells are initially confluent caudally with the mandibular arch ectomesenchyme, and it is still enigmatic how the mandibular ectomesenchyme is specified out of the trigeminal crest cells.

The craniofacial development of vertebrates is best understood from chick and mouse development. The chick system is especially advantageous for its experimental

[1] To whom correspondence should be addressed. Fax: +81-86-251-7876. E-mail: sasuke@cc.okayama-u.ac.jp.

0012-1606/00 $35.00

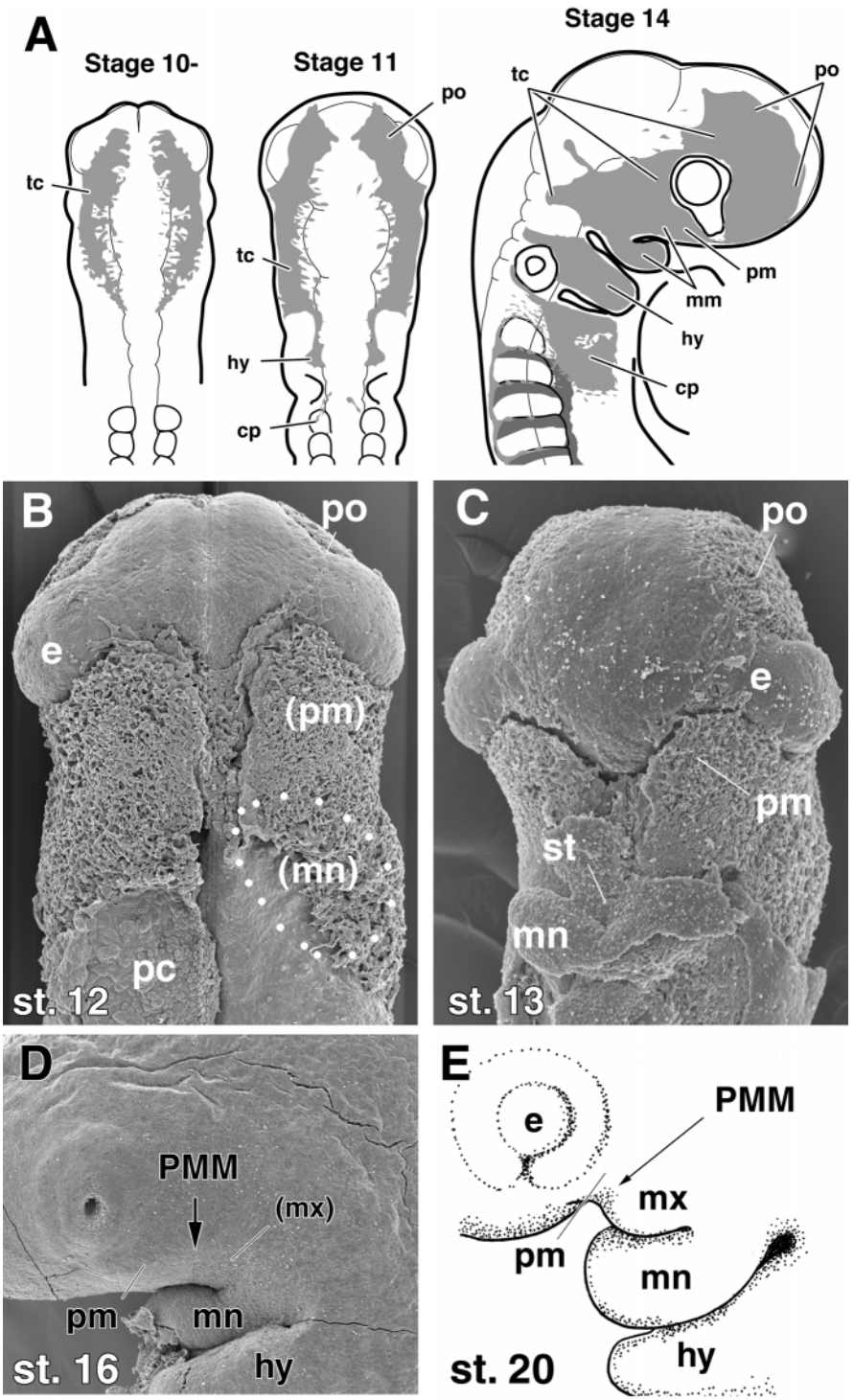


**FIG. 1.** Early distribution pattern of trigeminal crest cells in early chick embryos. (A) Schematic drawings of the cephalic crest cell distribution based on whole-mount HNK-1-immunostained embryos. Three populations of cephalic crest cells, trigeminal (tc), hyoid (hy), and circumpharyngeal (cp), are recognized in the stage 14 embryo. Of those, the trigeminal crest cells populate the maxillomandibular (mm) and premandibular (pm) regions of the head. (B–D) Scanning electron micrographs of stages 12 to 16 chick embryos. (B) Stage 12 embryo, ventral view. A sheet of crest cell covers the ventral aspect of the postoptic region of the head. This cell population covers the premandibular (pm) and maxillomandibular (mn) regions. Another crest cell subpopulation, or the preoptic cells (po), is seen on the dorsorostral aspect of the eye (e). Future maxillomandibular region is indicated by dots in (B). Labels in parentheses indicate the putativepremandibular and maxillomandibular regions. (C) Stage 13 embryo, ventral view. The mandibular processes have started

accessibility at the early embryonic period and for the availability of various molecular markers that show morphological identities. The present study was intended to show that there is a process of regionalization in the early rostral ectomesenchyme, before the appearance of pharyngeal arches, which is under the control of epithelially expressed growth factors. We also show that the above regionalization can be shifted by ectopic application of the growth factors as detected by the shift of craniofacial morphology and homeobox gene expressions.

## MATERIALS AND METHODS

### *Scanning Electron Microscopy*

Fertilized White Leghorn chicken eggs were incubated in a humid chamber at 38°C, and the embryos were staged according to Hamburger and Hamilton (1951). The embryos were fixed in 2.5% glutaraldehyde/0.1 M phosphate buffer (PB, pH 7.6), washed in PB, and postfixed with 4% osmium tetroxide/PB. The specimens were then rinsed in 0.1 M phosphate-buffered saline (PBS), and skinned with a sharpened tungsten needle. They were then dehydrated in a graded ethanol series and freeze-dried in *t*-butyl alcohol. Finally, the embryos were placed on an aluminum stub, sputter coated with gold–palladium alloy, and viewed by scanning electron microscopy (SEM; JSM-5800, JEOL, Peabody, MA).

### *Immunohistochemistry*

After fixation with 4% paraformaldehyde in 0.1 M PBS (PFA/PBS) at 4°C for 1 day, embryos were washed in 0.9% NaCl/distilled water, dehydrated in a graded series of methanol (50, 80, and 100%) and stored at −20°C. The samples were placed on ice in 2 ml dimethyl sulfoxide (DMSO)/methanol (1/1) until they sank. Five-hundred microliters of 10% Triton X-100/distilled water was added and the embryos were further incubated for 30 min at room temperature. After washing in Tris–HCl-buffered saline (TST; 20 mM Tris–HCl, pH 8.0; 150 mM NaCl; 0.1% Triton X-100), the samples were sequentially blocked with aqueous 1% periodic acid and with 5% nonfat dry milk in TST (TSTM). They were then incubated in the primary antibody 3A10 (Developmental Studies Hybridoma Bank, Iowa City, IA; diluted 1/100 in spin-clarified TSTM containing 0.1% sodium azide) for 2 to 4 days at room temperature while being gently agitated on a shaking platform. The secondary antibody used was horseradish peroxidase (HRP)-conjugated goat anti-mouse IgG (Zymed Lab. Inc., San Francisco, CA) diluted 1/200 in TSTM. After final washing in TST, the embryos were preincubated with the peroxidase substrates 3,3′-diaminobenzidine (DAB, 100 mg/ml) in TS for 1–2 h and allowed to react in TS with the same concentration of DAB with 0.004% hydrogen peroxide for 40 min at 4°C. The reaction was stopped and embryos were transferred simultaneously to a 30% glycerol/water mixture.

To observe the neural crest cell distribution, HNK-1 (Leu-7, Becton Dickinson, San Jose, CA) was used as the primary antibody. After being fixed with Bouin's fixative at 4°C for 1 h, embryos were washed and dehydrated in a graded series of ethanol and stored at 4°C. The subsequent procedures were the same as above, except that HRP-conjugated goat anti-mouse IgM (Zymed Lab. Inc.) was used as the secondary antibody and that TS containing 0.01% Triton X-100 was used for TST.

### *In Situ Hybridization*

For *in situ* hybridization, the embryos to be stained were fixed and stored in 1% PFA in PBS at 4°C. On the day before hybridization, the specimens were dehydrated and treated with 5% $H_2O_2$/methanol. The following steps and details have been described in Ogasawara *et al.* (2000). The double *in situ* hybridization was performed according to the method described by Funahashi *et al.* (1999).

### *Focal Injections of 1,1-Dioctadecyl-3,3,3′,3′-tetramethylindocarbocyanine Perchlorate (DiI)*

A window was cut through the eggshell and India ink, diluted 1/5 in 0.9% NaCl/distilled water, was injected into the subgerminal cavity to visualize the embryo. Embryos at Hamburger and Hamilton (1951) stages 8 to 9 were used for the injections into the neural crest. Using a fine glass pipette, a solution of DiI (Molecular probes, Eugene, OR) saturated in DMSO was injected onto the right side of the embryo at the forebrain to the midbrain neural crest. After the injection, a few drops of saline were applied to the embryo so that excess DiI solution was washed away. Embryos were then incubated further for 48 h and were fixed with 4% PFA/PBS for 2 h at room temperature. They were rinsed briefly with 0.9% NaCl and immersed in 30% glycerol/distilled water. The embryos were dissected and mounted on a depression slide glass and observed with fluorescence microscope. For injection into the ectomesenchyme of stage 13 embryos, the procedure was basically the same as above. These embryos were fixed 1 day after injections.

### *Growth Factor Bead Implantation*

Heparin beads (Sigma), soaked with mouse FGF8b (500 μg/ml, R&D Systems, Inc., Minneapolis, MN) and human BMP-4 (500 μg/ml, R&D Systems), were implanted into the interstices between ectoderm and mesenchyme in the presumptive premandibular region of stage 10 embryos (see Fig. 5A). After 2 days, the embryos were fixed and processed to analyze gene expression and morphology.

### *Whole Mount Staining of the Chondrocranium*

Operated embryos, sacrificed at stage 33, were fixed with 10% formalin in PBS. They were decapitated and skinned, and the eyes were removed. After washing in running tap water, they were fixed

protrusion. A siteof stomodaeum (st) is indicated. (D) Stage 16 embryo, lateral view. The PMM boundary is observed between the premandibular region and the putative maxillary process. As development proceeds, its boundary is as well defined to the anterior limit of the maxillary process. (E) Illustration of a stage 20 embryo to show the PMM boundary. Abbreviations: cp, circumpharyngeal crest cells; e, eye; hb, hindbrain; hy, hyoid crest cells or hyoid arch; mm, maxillomandibular region or mandibular arch; mn, mandibular process; pm, premandibular crest cell population; po, preoptic crest cell population; st, stomodaeum; tc, trigeminal crest cells.

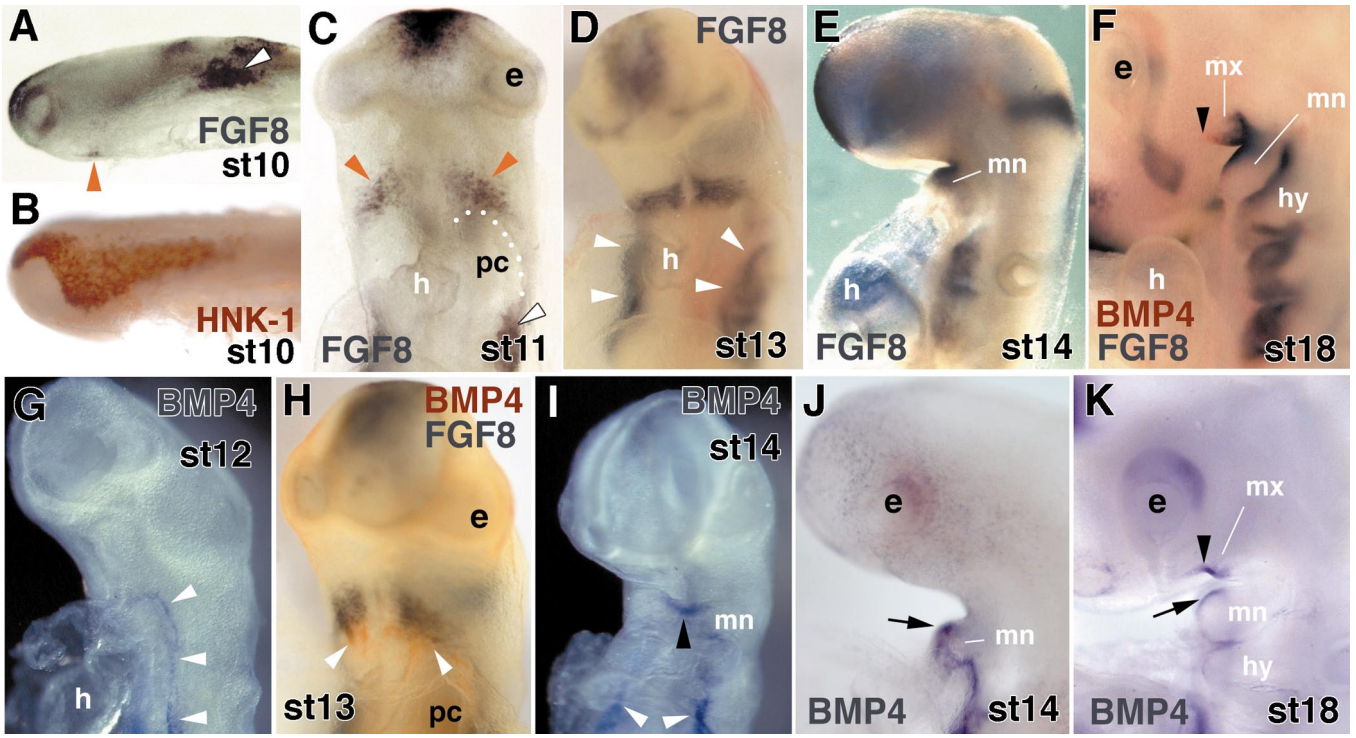


**FIG. 2.** Expression patterns of *Fgf8* and *Bmp4* in the early chick embryos. Developmental expression patterns of *Fgf8* (A, C–F, H), HNK-1 (B), and *Bmp4* (F–K). (A, B) Stage 10 embryos, lateral views. A faint expression domain of *Fgf8* is seen on the ventral ectoderm (orange arrowhead in A), prior to the influx of neural crest cells into the presumptive premandibular and mandibular regions (B). The white arrowhead in (A) indicates another expression domain in the caudal pharyngeal ectoderm. (C) Stage 11 embryo, ventral view. *Fgf8* expression has become distinct as a pair of patches in the ventral ectoderm (arrowheads) corresponding to the future maxillomandibular region. The caudal expression domain has also become distinct (white arrowhead). Contour of the pericardium (pc) is indicated by white dots. (D) By stage 13, the mandibular process has begun to protrude in the rostral expression domain of *Fgf8*, and the caudal expression has become divided into several independent domains (arrowheads). (E) Stage 14 embryo. *Fgf8* expression has been intensified at the root of the mandibular process (mn). (F) Stage 18 embryo. Maxillary (mx) and mandibular (mn) processes are distinct and the *Fgf8* expression domain is still seen on the ectoderm of both the processes. The caudal domains are restricted to the ectoderm of pharyngeal slits. An arrowhead indicates the PMM boundary. (G) *Bmp4* expression is faintly expressed first in the ventral portion of the pharyngeal ectoderm at stage 12 (arrowheads). (H) Double *in situ* hybridization with *Fgf8* and *Bmp4* riboprobes. The pharyngeal–ectodermal expression domain of *Bmp4* extends rostrally into the maxillomandibular expression domain (arrowheads), which partly overlaps with the *Fgf8* domain. (I) Stage 14 embryo. A black arrowhead indicates *Bmp4* expression in the mandibular arch ectoderm. White arrowheads indicate the ventral expression domain in the pharyngeal ectoderm. (J) Lateral view of another stage 14 embryo showing the mandibular expression (black arrow, also in K). (K) By stage 18, the *Bmp4* expression is intensified in the ectoderm at the PMM boundary, extending caudally into the maxillary process (mx). The caudal domain of *Bmp4* expression is restricted in the mandibular process ectoderm. Abbreviations: h, heart; hy, hyoid arch; mn, mandibular process; mx, maxillary process; pc, pericardium.

for 2 days in a solution containing 80% ethanol, 20% acetic acid, and 10 mg/liter Alcian blue. The embryos were washed in running water again and were digested with 1% trypsin in a mixture of three parts of saturated sodium tetraborate and seven parts of distilled water until the tissues became clear. The embryos were treated with 0.5% KOH and stored in 30% glycerol.

## RESULTS

### *Crest Cell Distribution Patterns and Craniofacial Morphology: Premandibular Crest Cells*

Three major populations of cephalic crest cells stained with the HNK-1 antibody in the chick embryonic head (Fig. 1A). These are, from rostral to caudal, the trigeminal, hyoid, and circumpharyngeal crest cells (reviewed by Kuratani and Kirby, 1991; Shigetani *et al.*, 1995; Kuratani, 1997). Of these, the trigeminal crest cells populated the ventral aspect of the head rostral to the pericardium at stage 12 as a continuous sheet of cells (Fig. 1B). The hyoid and circumpharyngeal crest cells formed the ectomesenchyme in the second arch and in the postotic pharyngeal arches, respectively. The mandibular process appeared at stage 13 as a swelling of the caudal portion of the trigeminal crest cells (Fig. 1C). There was no apparent distinction in the ventral cell population of the trigeminal crest cells to separate the premandibular cells from

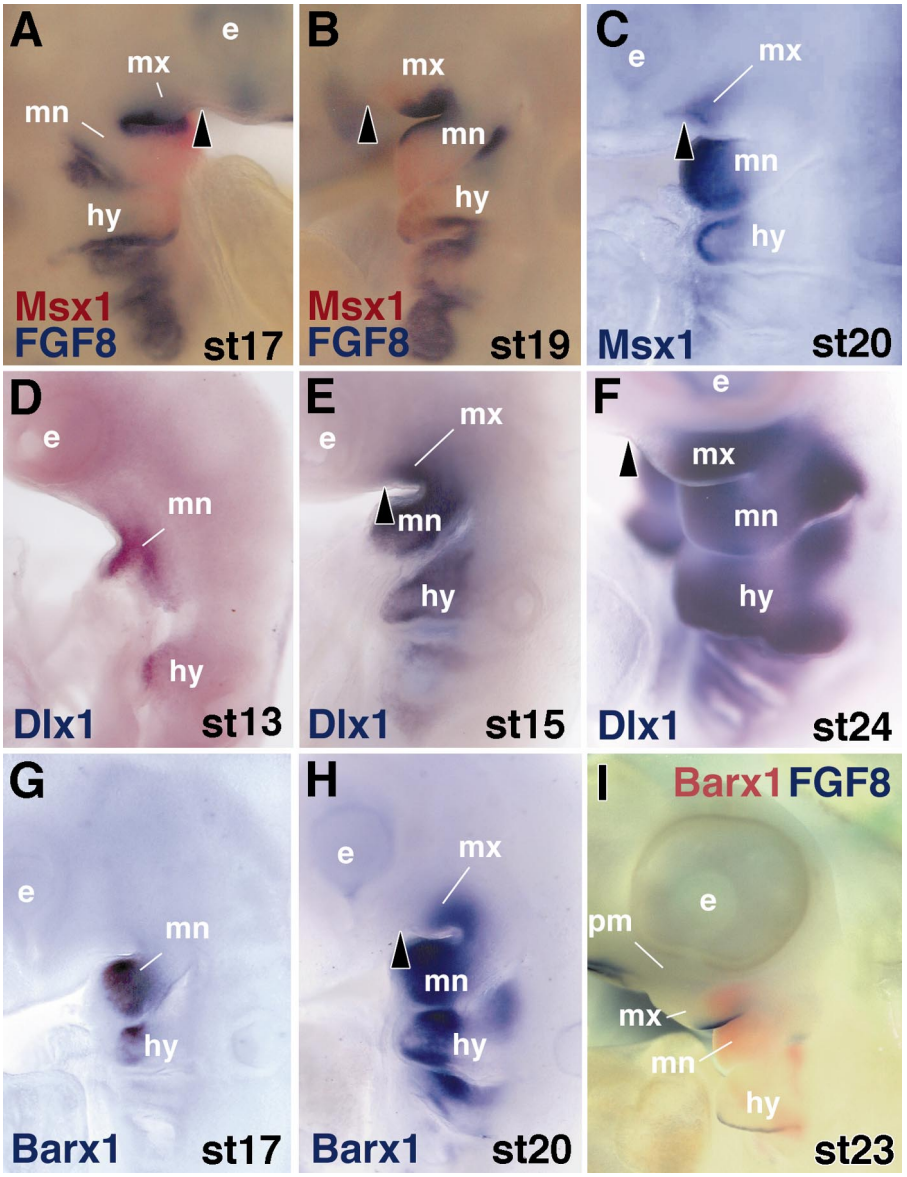


**FIG. 3.** Expression patterns of mesenchymally expressed homeobox genes in the chick embryos. In all the figures, black arrowheads show the PMM boundary. (A–C) Expression patterns of *Msx1*. (A, B) Double *in situ* hybridization with *Msx1* and *Fgf8* riboprobes. Note that the *Msx1* expression domains in the maxillary and mandibular mesenchyme overlap that of *Fgf8* expression in the ectoderm. (B) At stage 19, *Msx1* is first upregulated in the premandibular–maxillary transitional area as well as in the ventral part of the mandibular arch. (C) At stage 20, the expression of *Msx1* in PMM transitional area is intensified. (D–F) Expression patterns of *Dlx1*. Stage 13 embryo (D) shows the earliest expression pattern of *Dlx1*. In the mandibular arch, the expression domain is restricted to the mesenchyme, never extending rostrally beyond the PMM boundary (E, F). (G–I) Expression patterns of *Barx1*. Similar to *Dlx1*, *Barx1* expression is restricted to the pharyngeal arch mesenchyme, but is delayed compared to that of *Dlx1*. Abbreviations: hy, hyoid arch; mn, mandibular process; mx, maxillary process.

those in the mandibular arch (Figs. 1B and 1C). The rostral part of this cell population will be referred to as premandibular crest cells from its position, and the posterior, the putative maxillomandibular crest cells (Figs. 1C–1E). By stage 16, the rostral edge of the putative maxillary process had developed an indentation delineating the maxillomandibular region from the premandibular (premandibular–maxillomandibular boundary (PMM boundary below); Figs. 1D and 1E). The premandibular and maxillomandibular regions are thus derived from continuous trigeminal crest cells through secondary partitioning and are not established independently.

### *Regulatory Gene Expression Patterns in the Early Chick Embryo*

Before the appearance of the mandibular arch, several growth-factor-encoding genes are already expressed in the head ectoderm. *Fgf8* transcripts appeared as early as stage 10 in the ventral surface ectoderm (Fig. 2A), before the influx of neural crest cells into the presumptive mandibular arch region (Fig. 2B; cf. Fig. 1). As development proceeded, these paired expression domains remained in the ectoderm of angular portions of the mandibular arch (Figs. 2C–2F and 2H). Caudally, another *Fgf8* expression domain was seen in the future pharyngeal ectoderm as a pair of bands lateral to the pericardium (Figs. 2A, 2C, and 2D). Expression of *Bmp4* was also seen in the mandibular and pharyngeal ectoderm, in domains adjacent to those of *Fgf8* (Figs. 2F–2K). It was expressed along the pericardium (Figs. 2G–2I) and was later found in the distal tips of the mandibular arch (Figs. 2F and 2I–2K). Notably, a new expression domain of *Bmp4* had appeared in the distal part of the maxillary process by stage 18 (Fig. 2K). It began before the appearance of an indentation that demarcated the maxillary process from the premandibular region (data not shown). Thus, in the ventral head ectoderm, *Fgf8* expression was primarily associated with the mandibular region, and those of *Bmp4* surrounded the *Fgf8* domains.

The ectodermal expression of the growth factors as shown above were coextensive with those of some homeobox genes that are localized in specific parts of the ectomesenchyme. *Msx1*, the downstream target of BMP4, was first upregulated in the ventral mesenchyme in the mandibular process and then expressed in the maxillary process and the more rostral region beyond the PMM boundary (Figs. 1 and 3A–3C). This is similar to the ectodermal expression of *Bmp4* (Fig. 2K). *Dlx1*, a target of FGF8, was expressed throughout the ectomesenchyme of the mandibular arch (Figs. 3D–3F: compare with Figs. 2D–2F). *Barx1* was expressed slightly later than, and in a similar pattern to, *Dlx1* (Figs. 3G–3I). Their expression patterns suggest that FGF8 and BMP4 are involved in the specification of the mandibular arch ectomesenchyme out of the trigeminal crest cells; ectodermally expressed growth factor serves as a prepattern for the apparently homogenous trigeminal ectomesenchyme by inducing local expressions of the target homeobox genes (Fig. 4).

### *Ectopic Applications of FGF8 Change the Fate of Premandibular Crest Cells into Mandibular Crest Cells*

If localized expression of the growth factors are responsible for the premandibular–mandibular specification, will the ectopic application of these factors alter the pattern of facial primordia? To address this question, we performed local application of beads soaked with either mouse FGF8 or human BMP4 recombinants into the putative premandibular region at stage 10. At this stage, mesenchymal expression of the homeobox genes was not yet observed and no apparent regionalization of premandibular and maxillomandibular regions was apparent (Fig. 4).

After an FGF8 bead was implanted into the presumptive postoptic region, *Barx1* expression also expanded rostrally as well as dorsally (Fig. 5C: compare with Fig. 5B). The premandibular region was smaller, the eye was reduced in size, and its lens shifted slightly posteriorly (Fig. 5C). The morphological identity of each mesenchymal region is reflected partly by the peripheral nerve morphology that mirrors the local identities of cranial neural crest cells (Johnston, 1966; Noden, 1975). We therefore observed the trigeminal nerve morphology by immunostaining of the embryos with implanted FGF8 beads with the neurofilament-specific antibody, 3A10. Normally, the embryonic trigeminal nerve bifurcates distally into the ophthalmic nerve that innervates the rostral and caudal aspects of the eye as well as the frontonasal region and the maxillomandibular nerve that grows into the mandibular arch and its derivatives (Fig. 5D). Implantation of an FGF8 bead disturbed the morphology of the trigeminal nerve (Fig. 5E). The ophthalmic branch that normally supplies the posterior aspect of the eye was reduced, and some ramules grew from the maxillomandibular nerve into the region, which otherwise is innervated by the ophthalmic nerve (Fig. 5E). This morphological change implies that the identity of the postoptic (=premandibular) region might have been altered into that of the maxillomandibular region.

### *Transformation of the Crest Cells*

To examine the behavior of crest cells after the implantation of an FGF8 bead, immunolabeling and DiI labeling of the crest cells were performed. By immunostaining the embryos with HNK-1, the marker of neural crest cells, early migrating cells in the premandibular and mandibular regions could be observed 1 day after bead implantation. No change was detected in the distribution of the trigeminal crest cells between the bead-implanted and control sides (data not shown), implying that the bead did not affect the initial migration and distribution patterns of the crest cells in the rostral head. We focused, therefore, on later stages by observing the embryos 2 days after the focal injection of DiI at stages 8 to 9. The sites of injection were determined after the experiment on observing from the progression of the dye along the central nervous system. Normally, the forebrain and anterior midbrain crest cells preferentially populate the premandibular region (13 of 13 embryos, each; Table 1), although a few labeled cells were also observed in the mandibular region (0 of 13 and 4 of 13 embryos; Table 1). The posterior midbrain-derived crest cells, on the other hand, mostly populated the mandibular arch derivatives (9 of 9 embryos; Table 1) as already described in amniote embryos (Osumi-Yamashita *et al.*, 1994; Köntges and Lumsden, 1996). Thus, the neural crest at the fore- and midbrain levels was likely to be roughly organized into

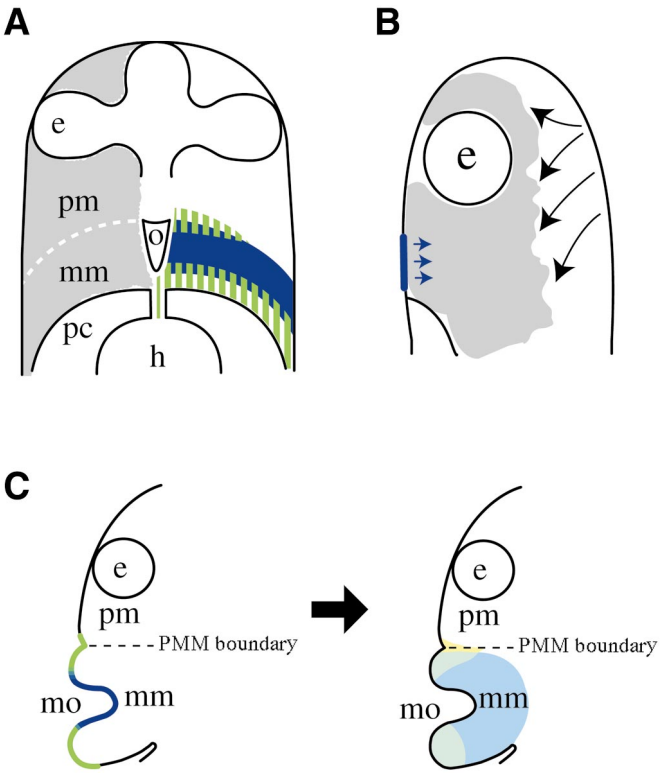


**FIG. 4.** Diagram of expression patterns of *Fgf8* and *Bmp4* and suggested mechanism for regionalization of the trigeminal ectomesenchyme. (A) Chick embryonic head, ventral view. The left side shows the future specification of the cephalic crest cells (gray), which corresponds to the ectodermal expression domains of *Fgf8* (blue) and *Bmp4* (green vertical lines) on the right. *Fgf8* is first expressed as a pair of patches prefiguring the maxillomandibular region. A median negative region, corresponding to the putative oral ectoderm (o) separates them. *Bmp4* is expressed around the pericardium (pc) and in the PMM boundary. (B) An early embryo, lateral view. Trigeminal crest cells (gray) emigrate from fore- and midbrain levels and are distributed ubiquitously in the premandibular and maxillomandibular regions. FGF8 signals (blue) are thought to induce the identity of the maxillomandibular region out of this ectomesenchyme. (C) Later stage embryos, lateral views. (Left) The indentation rostral to the maxillomandibular region (PMM boundary) is formed at the rostral *Bmp4* expression domain. *Fgf8* and *Bmp4* expression domains are colored blue and green, respectively. (Right) Homeobox gene expression patterns. *Dlx1* and *Barx1* are expressed in the whole mandibular arch (light blue). *Msx1* is expressed at the PMM boundary (yellowish-green). Overlapped expression domains are colored with bluish-green in the distal tips of maxillary and mandibular processes. Abbreviations: e, eye; h, heart; mo, mouth; PMM boundary, premandibular–maxillomandibular boundary.

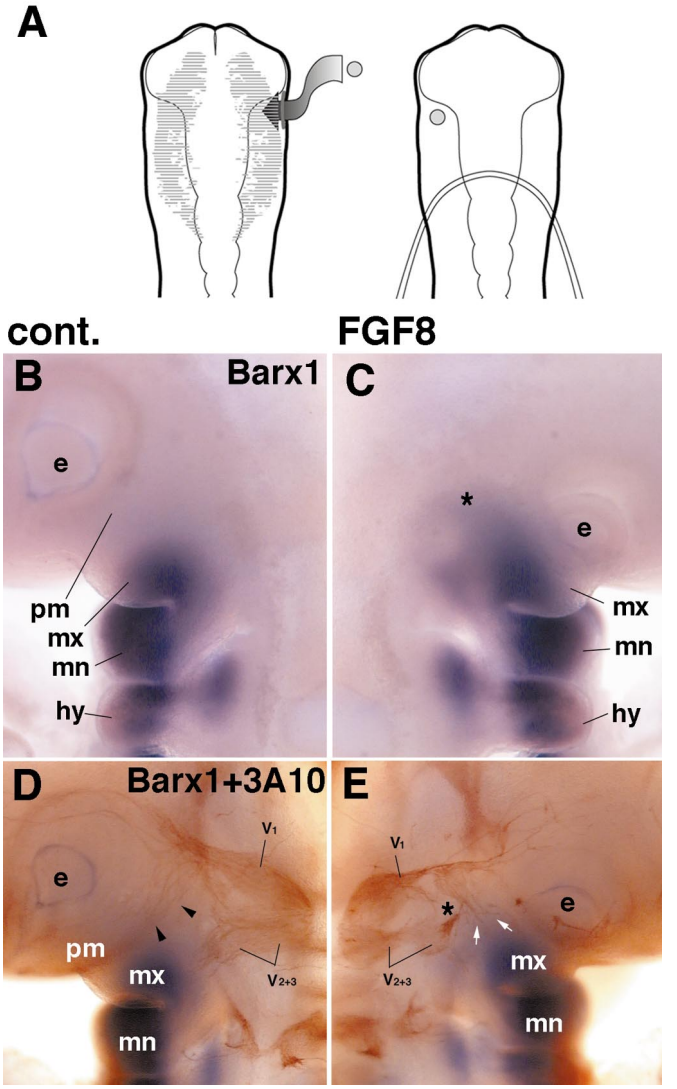


**FIG. 5.** FGF8 beads implantations. (A) The experimental procedure. A slit was made on the right lateral surface ectoderm of the embryo (left, dorsal view) and the bead was inserted ventrally into the presumptive premandibular region (right, ventral view). (B–E) An embryo that received an FGF8-soaked bead. (B, C) *Barx1* expression patterns 48 h after implantation. The control (B) and the operated sides (C). By ectopic application of FGF8 (the bead site is indicated by asterisk), *Barx1* expression is expanded in the experimental side (C). Note that the eye is reduced on the operated side of the embryo. (D, E) Trigeminal nerve morphology. The same embryo shown in (B) and (C) has been immunohistochemically stained with the monoclonal antibody, 3A10. (D) The trigeminal nerve normally consists of the ophthalmic nerve (V1) that innervates the eye (e) and premandibular region (indicated by arrowheads) and the maxillomandibular nerve (V2+3) in the mandibular arch (mx and mn). Note that the latter nerve is restricted to the *Barx1*-expressing domains. (E) By ectopic application of FGF8 (asterisk), the mesenchymal region caudal to the eye (indicated by white arrows) receives fibers from both the maxillomandibular and ophthalmic nerves. This region is normally innervated only by a ventral branch of the ophthalmic nerve (arrowheads in D). Abbreviations: e, eye; hy, hyoid arch; mn, mandibular process; mx, maxillary process; pm, premandibular region.

mandibular and premandibular subpopulations (Table 1). The results were the same when PBS-soaked beads were implanted after the DiI injection (Table 1 and Fig. 6A). After implantation of the FGF8 beads, DiI labeling revealed a major population of the anterior midbrain-derived crest

**TABLE 1**
The Distribution Pattern of DiI-Labeled Trigeminal Crest Cells after FGF8 Bead Implantation

| Sites of DiI injections and types of bead implantations | Embryos with labeled cells in the premandibular region/total embryos observed | Embryos with labeled cells in the mandibular region/total embryos observed |
|---|---|---|
| Diencephalon | | |
| No bead | 13/13 | 0/13 |
| Anterior midbrain | | |
| No bead | 13/13 | 4[a]/13 |
| PBS bead | 9/9 | 0/9 |
| FGF8 bead | 10/10 | 10/10 |
| Posterior midbrain | | |
| No bead | 5 + 1[a]/9 | 9/9 |

*Note.* The anterior midbrain can contain the level of the diencephalic–mesencephalic boundary, and the posterior midbrain, the isthmus. The injections into the middle one-third of the midbrain were not counted in the above list.

[a] Only a few cells were found in the indicated regions.

cells both in the reduced premandibular region and in the apparent mandibular region in all the embryos (10 of 10 embryos; Table 1 and Fig. 6B). We conclude, therefore, that at least a part of the ventral trigeminal crest cells, which would have differentiated into the premandibular identity, was transformed into the identity of the mandibular arch by ectopic FGF8.

At stage 13 of normal embryos, in which the PMM boundary is not clearly observed, focal injections of DiI were also performed into the local ectomesenchyme of the trigeminal region (Fig. 6C). Labeled cells always grew as continuous masses of cells, and only a few labeled cells moved across the PMM boundary (Figs. 6D–6F). It seems likely, therefore, that by stage 13 the trigeminal crest cells are already specified into premandibular, maxillomandibular, and possibly the preoptic subpopulations. No active movement appears to take place between each of the domains. Local interactions between the ectoderm and the mesenchyme thus may involve stable positioning of the crest cells, which is roughly fixed at least by stage 13.

### *Ectopic BMP4 Eliminates the Maxillomandibular Region*

In the normal ectoderm, the rostral expression domain of *Bmp4* appears as if it might limit the expansion of the *Fgf8* expression domain (Figs. 2F and 2K). To test this possibility, BMP4-soaked bead implantation was performed. Contrary to the FGF8 bead implantation, this experiment resulted in the reduction of the maxillomandibular portion and of the domain of *Dlx1* expression (Figs. 5F–5I). Almost all of the mandibular arch disappeared on the operated side, but the posterior and anterior (maxillary) portions usually remained (Fig. 5G). Unexpectedly, ectopic BMP4 application arrested development of the entire trigeminal nerve complex (including the maxillomandibular and ophthalmic nerves; Figs. 5H and 5I); all the peripheral branches failed to develop and only the trigeminal ganglion was present (Fig. 5I).

Some of the operated embryos were stained in whole mount with Alcian blue to observe the chondrocranial morphology. In the embryos that had received the BMP4 bead, Meckel's cartilage was totally lost on the experimental side (2 of 5 embryos, Fig. 7A), while the retroarticular process, which has been shown to be of the second arch origin (Köntges and Lumsden, 1996), was fused with the quadrate cartilage (Fig. 7C). No change occurred in the putative premandibular skeletal elements, such as the interorbital septum, trabecular cartilage, or basitrabecular process (de Beer, 1937; Couly *et al.*, 1993), except that the articulation between the quadrate and basitrabecular process was lost on the experimental side (Figs. 7B and 7C).

## DISCUSSION

### *Specification of the Trigeminal Crest Cells*

The present study has shown that the anterior cephalic crest cells are first distributed ubiquitously in the premandibular and maxillomandibular regions of early chick embryos, with no obvious boundaries (Figs. 1B and 1C). For the most rostral cephalic crest cells that cover the trigeminal region, mapping of premigratory neural crest cells has not been well studied. This is partly because the premandibular region has often been confused with the maxillary region that is a part of the mandibular arch. Considering the premandibular regions, however, the literature seems to show that crest cell streams can be roughly mapped to two regions. First, those in the posterior midbrain give rise to mandibular arch cells. Second, as we found, cells in the anterior midbrain and more rostral neural crest migrate mostly into preoptic and premandibular regions (Osumi-Yamashita *et al.*, 1994).

Unlike the more caudal pharyngeal arches, in which the genetic code is strongly precommitted along the neuraxis and crest cell streams are well dissociated from each other by r3 and r5 regions (Lumsden *et al.*, 1991), the ectomesenchyme in the trigeminal region appears to be only roughly specified anteroposteriorly in the premigratory neural crest at the midbrain and forebrain levels. As suggested in the present study, later specification rather depends on ectodermally derived signals including FGF8 and BMP4; locally established ectodermal–ectomesenchymal tissue interactions appear to regionalize the premandibular and mandibular regions out of this apparently homogenous cell population. This premandibular–mandibular patterning, which precedes the proximodistal patterning within the mandibular arch, is apparently able to respecify by the change of ectodermally expressed growth factors, FGF8 and BMP4. The present experiments have actually shown that the local identities of the premandibular and mandibular ectomesen-

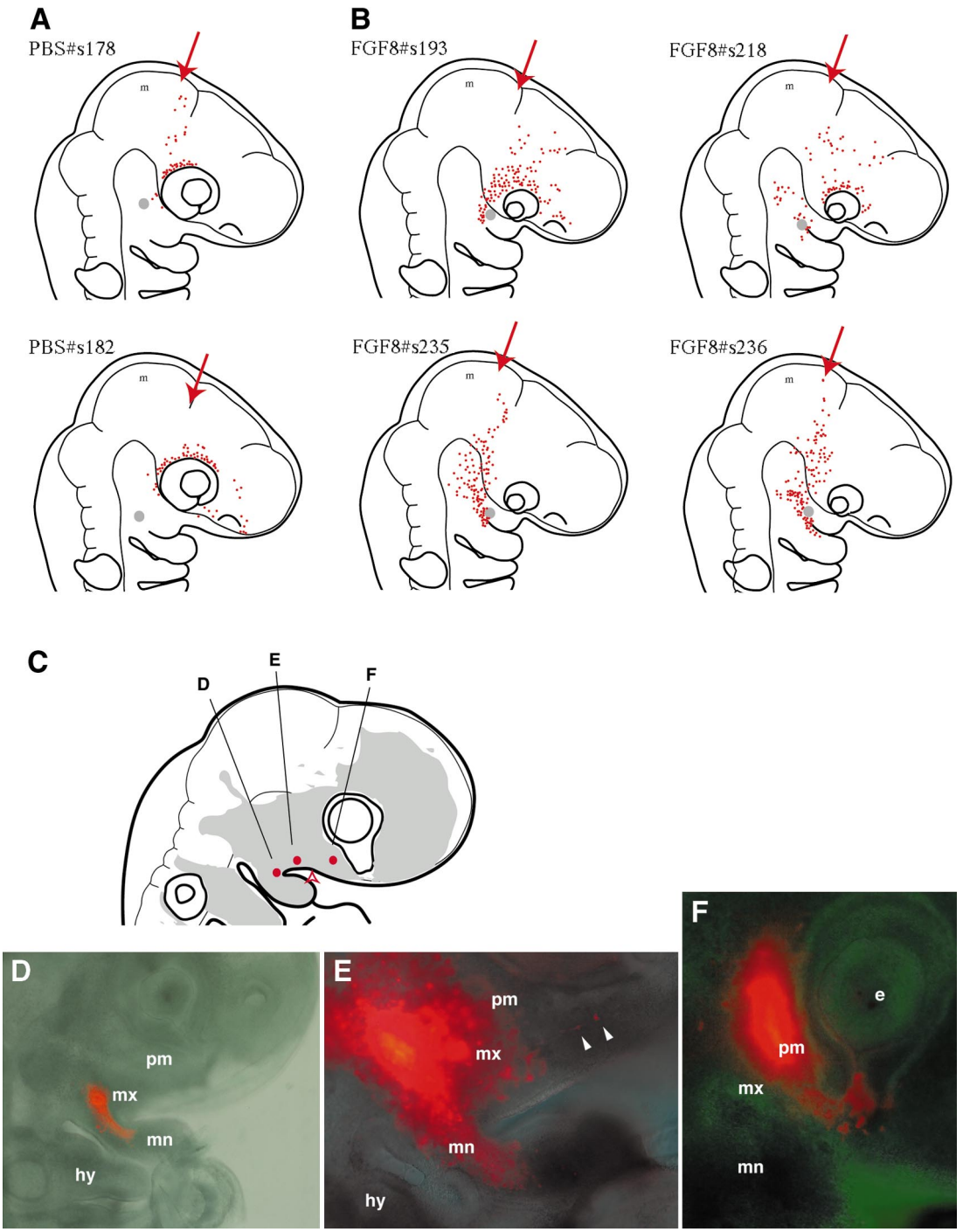


**FIG. 6.** Focal injection of DiI into the trigeminal crest cells. (A, B) Mapping of the premandibular crest cells. (A) Sham-operated embryos that received PBS-soaked beads after focal injections of the neural crest with DiI. Note that most of the rostral midbrain-derived crest cells populate the premandibular region. Similar labeling was obtained in control embryos in which beads were not implanted. (B) Four examples of DiI-injected embryos that received FGF8 beads after the injection. Many of the labeled cells have populated the rostrally shifted maxillary process which would have had developed into the premandibular region in normal development. (C–F) Local specification of the trigeminal ectomesenchyme after stage 13. (C) Injections were made into three different sites (small D to F) of the ectomesenchyme at stage 13 when the PMM boundary is faintly visible. The open arrowhead indicates the presumptive site of the PMM boundary. (D) Labeled cells are mostly distributed as a continuous band of cells that runs along the axis of the mandibular arch. (E) The maxillary and mandibular mesenchymes are labeled as a single mass. Only a few cells are migrating into the premandibular domain. (F) Premandibular injection results in the rostral growth of labeled cells. Some of the labeled cells are adhering to the ventral aspect of the optic nerve.

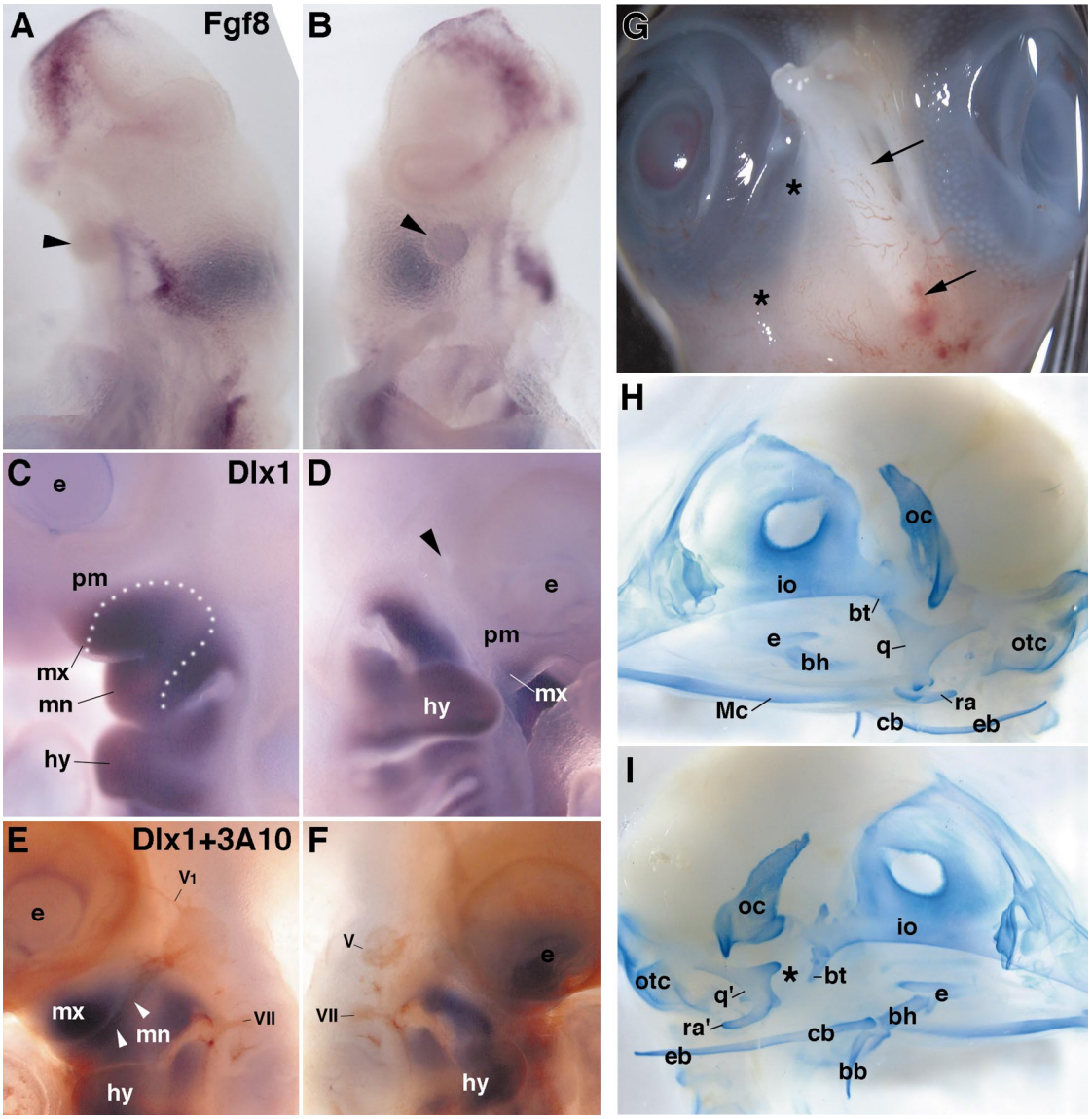


**FIG. 7.** BMP4 beads implantations and cranial development. The experimental procedure was similar to that for FGF8 bead implantation (Fig. 5A). (A, B) *Fgf8* expression patterns on the control (A) and operated (B) sides of an embryo 6 h after the bead implantation. Arrowheads indicate the implanted beads. The ectodermal expression of *Fgf8* is completely lost on the experimental side (B). A large bead was used for this particular embryo. (C, D) Expression of *Dlx1* on the control (C) and the experimental (D) sides of the embryo 48 h after implantation. Expression domain of *Dlx1*, or the mandibular arch region, is reduced on the experimental side (D). Note in (D) that the periangular part of the mandibular arch is entirely missing. Arrowhead indicates the site of bead implantation. This lost portion corresponds to the region indicated by white dots in (C). (E, F) Another embryo hybridized *in situ* for *Dlx1* expression (dark purple portions) and immunostained with the monoclonal antibody, 3A10 (dark orange). On the control side (E), the trigeminal nerve has grown the ophthalmic nerve (V1) rostrally and the maxillomandibular nerve (arrowheads) into the mandibular arch. On the operated side (F), all the trigeminal peripheral branches are arrested. (G) The ventral view of stage 33 embryo in which BMP4 bead had been implanted onto the right side of the PMM boundary region at stage 10. The left half of the lower jaw has developed normally on the left side (arrows), but the right half is absent (asterisks indicate the position where the lower jaw is expected). (H) The control side of the same embryo as shown in (G). Whole mount stained with Alcian blue. The cartilage of Meckel (Mc) and quadrate (q) are the derivatives of the mandibular arch. The quadrate articulates with the cranial base by means of the basitrabecular process (bt). The caudal end of the cartilage of Meckel continues into the retroarticular process (ra), which has been shown to be of hyoid arch derivative (Köntges and Lumsden, 1996). (I) The experimental side of the same embryo. Meckel's cartilage is absent, but the retroarticular process-like cartilage is fused with the quadrate (q′) that does not articulate with the basitrabecular process (asterisk). Abbreviations: bb, basibranchial; bh, basihyal; bt, basitrabecular process; cb, ceratobranchial; e, entoglossum; eb, epibranchial; io, interorbital cartilage; Mc, Meckel's cartilage; oc, orbital capsule; otc, otic capsule; q, quadrate; ra, retroarticular process.

chyme can be shifted by local application of growth factors. The repatterning of the premandibular and mandibular region was consistent with the changed expression pattern of presumed target genes of FGF8 and BMP4. Importantly, the rostrally shifted position of the maxillary process by FGF8 reflects, at least in part, the transformation of the crest cells that otherwise would have developed into the premandibular identity (Table 1, Fig. 1).

### *FGF–BMP Signaling and Ectomesenchymal Patterning*

In the differentiation of the mandibular arch, the roles of FGFs and BMPs have been emphasized recently as the upstream factors of local regulation of the mesenchymally expressed genes, which specify the polarities of the arch mesenchyme (Barlow and Francis-West, 1997; Tucker *et al.*, 1998a,b, 1999a,b; Thomas *et al.*, 2000; Ferguson *et al.*, 2000). These experiments focused on rather late developmental patterning that is restricted within the domain of the mandibular arch. These growth factors have been postulated to be involved in the proximodistal patterning of the mandibular arch (Neubüsser *et al.*, 1997; Thomas *et al.*, 2000). The present experiments have shown that similar sets of molecular cascades are used in the earlier patterning event on which the mandibular arch patterning is dependent. In this context, the morphology of the BMP4 bead-implanted embryo (Fig. 7) is reminiscent of a murine transgenic experiment, in which *Fgf8* was inactivated by the *Cre/loxP* system (Trumpp *et al.*, 1999). The loss of FGF8 in the latter experiment may have been to a similar time table to ours, as it seems the initial regionalization of the mandibular arch was arrested in this transgenic mouse. Craniofacial patterning thus appears to be sequential series of inductive events between the ventral ectoderm and the ectomesenchyme. In particular, ectodermal localization of FGF8 was assumed to function in the initial regionalization of the mandibular arch crest cells out of the trigeminal crest cells. Expression of *Fgf8* precedes the influx of crest cells into the pharynx, implying that the basic morphological plan of the craniofacial region is set up early in the surface ectoderm.

One of the basic mechanisms behind the above patterning process would be the balanced and stabilized expression domains of *Fgf8* and *Bmp4*. As already reported, FGFs and BMPs act in an antagonistic fashion (Neubüser *et al.*, 1997; Ericson *et al.*, 1998; Tucker *et al.*, 1998a). Similar mechanisms may also be involved in PMM regionalization. In the early phase of mandibular arch specification, our experiments as well as the normal expression sequence of these genes imply that BMP4 may limit *Fgf8* expression and secondarily repress *Dlx1* expression, which eventually reduces part of the mandibular arch (Fig. 7D). Actually, the *Dlx1* expression domain lost by the BMP4 bead implantation (Figs. 7C and 7D) corresponds exactly to the region where *Dlx1* is thought to be upregulated only by FGF8 (Fig. 8). Such an interaction would be a part of stabilized local expression patterns of the regulatory genes in the craniofacial region (Fig. 8). Probably, early expression domain of *Fgf8* can be regarded as the ectodermal portion to define the mandibular arch, which secondarily regionalizes also the PMM boundary.

The regulatory mechanism between BMP4 and FGF8 remains unclear. The equilibrium between FGF8 and BMP4 may also be mediated by the underlying mesenchyme, as shown in the murine mandibular arch (Thomas *et al.*, 2000). The interaction may not be simple either; ectopic FGF8 not only induces *Bmp4*, but it can also repress *Bmp4*, as seen in the eye. This may possibly be regarded as a secondary effect, since the involvement of BMP4 in the normal development of the retina and lens has been shown in the mouse (Furuta and Hogan, 1998). We conclude, in the present study, that the FGF8 and BMP4 genes are involved in the early patterning of the craniofacial region that separates the maxillomandibular region against the more rostral part of neural-crest-filled region or the premandibular region. The latter region has been neglected so far in developmental biology.

After the implantation of BMP4 and FGF8 beads, the HNK-1 immunostaining did not show any overt disruption of the crest cell distribution (data not shown). The shifts of the expression of homeobox genes and subsequent change of regionalization are therefore not due to cell migration, but are more likely to be due to the early change of growth factor distribution that altered mesenchymal expression of the target genes. Initial regionalization and specification of unsegmented trigeminal crest cells thus seem to be established through tissue interactions between crest cells and surface ectoderm. In addition, this association must take place within a narrow window of timetable before stage 13, since the shift of patterning is restricted within the mandibular arch when the growth factor beads are implanted at later stage of development, as noted above (Thomas *et al.*, 2000; Ferguson *et al.*, 2000). The loss of mandibular-arch-derived cartilage by ectopic BMP4 is consistent with our hypothesis. The most striking effect was the absence of the cartilage of Meckel, which never occurs when similar experiments are carried out on later stage embryos. The quadrate cartilage in older embryos (Fig. 7I) might have derived from such a remainder of the maxillary process, as seen in Fig. 7D. In our experiments, it was not possible to determine how long the ectopic growth factor could affect the regulation of homeobox genes. Furthermore, it has recently been found that the mesenchymal expression of the homeobox genes does not require the presence of the epithelium after a certain stage of development (Ferguson *et al.*, 2000). This might explain the partial development of the mandibular arch in our experiment.

In conclusion, FGF8 (probably in association with BMP4) is most likely to be involved in the partitioning of the trigeminal crest cells into premandibular and mandibular regions, through epithelial–mesenchymal interactions. In later development, the same molecular cascades are used in patterning within the mandibular arch, as stated by previ-

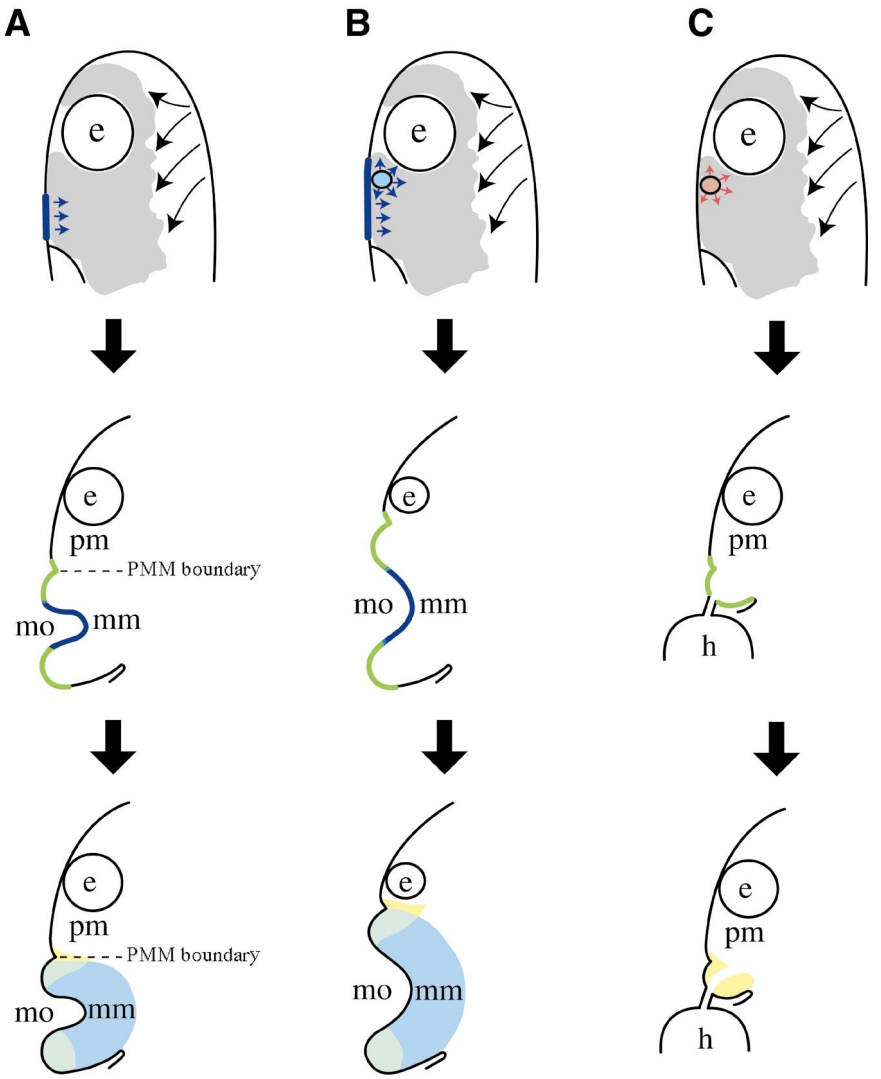


**FIG. 8.** Models for the PMM patterning mechanisms by FGF8 and BMP4. (A) Normal development. Ectodermally derived FGF8 induces the maxillomandibular region in the caudal part of the trigeminal ectomesenchyme, the identity of which is shown by *Dlx1* and *Barx1*. (B) FGF8-bead-implanted embryos. By enhanced amount of FGF8, a larger domain of trigeminal ectomesenchyme is patterned as the maxillomandibular region and the PMM boundary shifts rostrally. This appears to involve the transformation of the original premandibular region into the identity of the maxillomandibular. (C) BMP4-bead-implanted embryos. BMP4 appears to suppress the expression of FGF8, resulting in the disappearance of the maxillomandibular identity that is defined by FGF8. Remnants of the mandibular arch correspond to the parts which normally develop from BMP4 expressing regions. Abbreviations: e, eye; h, heart; mm, maxillomandibular region; mo, mouth opening; pm, premandibular region; PMM boundary, premandibular–maxillomandibular boundary.

ous authors. It is curious that the same molecular mechanisms function in different phases of the hierarchically constructed, craniofacial developmental program, being expressed in the fixed position in the embryonic ectoderm.

## ACKNOWLEDGMENTS

The 3A10 antibody developed by Dr. T. Jessell was obtained from the Developmental Studies Hybridoma Bank maintained by the Department of Pharmacology and Molecular Sciences, Johns Hopkins University School of Medicine, Baltimore, Maryland, and the Department of Biological Sciences, University of Iowa, Iowa City, Iowa, under Contract N01-HD-2-3144 from the NICHD. We are grateful to Isato Araki, Harukazu Nakamura, Tsutomu Nohno, Chikara Hashimoto, Kenji Shimamura, John Rubenstein, and Philippa Francis-West, for their gift of cDNA probes. We also thank Ruth T. Yu for her critical reading of the manuscript and valuable discussion and Kazuko Koshiba for her technical advice. This work has been supported by JSPS Research Fellowship for Young Scientists to Y.S. and by Grants-

in-Aid from the Ministry of Education, Science and Culture of Japan to S.K. (Grants 11309010, 11NP0201, and 11152225).

## REFERENCES

Barlow, A. J., and Francis-West, P. H. (1997). Ectopic application of recombinant BMP-2 and BMP-4 can change patterning of developing chick facial primordia. *Development* **124,** 391–398.

Barlow, A. J., Bogardi, J. P., Ladher, R., and Francis-West, P. H. (1999). Expression of chick *Barx-1* and its defferential regulation by FGF-8 and BMP4 signaling in the maxillary primordia. *Dev. Dyn.* **214,** 291–302.

Bei, M., and Maas, R. (1998). FGFs and BMP4 induce both *Msx1*-independent and *Msx1*-dependent signaling pathways in early tooth development. *Development* **125,** 4325–4333.

Couly, F. C., Coltey, P. M., and Le Douarin, N. M. (1993). The triple origin of skull in higher vertebrates: A study in quail–chick chimeras. *Development* **117,** 409–429.

de Beer, G. R. (1937). "The Development of the Vertebrate Skull." Oxford Univ. Press, London.

Ericson, J., Norlin, S., Jessel, T. M., and Edlund, T. (1998). Integrated FGF and BMP signaling controls the progression of progenitor cell differentiation and the emergence of pattern in the embryonic anterior pituitary. *Development* **125,** 1005–1015.

Ferguson, C. A., Tucker, A. S., and Sharpe, P. T. (2000). Temporospatial cell interactions regulating mandibular and maxillary arch patterning. *Development* **127,** 403–412.

Funahashi, J., Okafuji, T., Ohuchi, H., Noji, S., Tanaka, H., and Nakamura, H. (1999). Role of *Pax-5* in the regulation of a mid-hindbrain organizer's activity. *Dev. Growth Differ.* **41,** 59–72.

Furuta, Y., and Hogan, B. L. M. (1998). BMP4 is essential for lens induction in the mouse embryo. *Genes Dev.* **12,** 3764–3775.

Hamburger, V., and Hamilton, H. L. (1951). A series of normal stages in the development of the chick embryo. *J. Morphol.* **88,** 49–67.

Johnston, M. C. (1966). A radioautographic study of the migration and fate of cranial neural crest cells in the chick embryo. *Anat. Rec.* **156,** 143–155.

Köntges, G., and Lumsden, A. (1996). Phombencephalic neural crest segmentation is preserved throughout craniofacial ontogeny. *Development* **122,** 3229–3242.

Kuratani, S. C., and Kirby, M. L. (1991). Initial migration and distribution of the cardiac neural crest in the avian embryo: An introduction to the concept of the circumpharyngeal crest. *Am. J. Anat.* **191,** 215–227.

Kuratani, S. (1997). Distribution of postotic crest cells in the chick embryo defines the trunk/head interface: Embryological interpretation of crest cell distribution and evolution of the vertebrate head. *Anat. Embryol.* **195,** 1–13.

Lumsden, A., Sprawson, N., and Graham, A. (1991). Segmental origin and migration of neural crest cells in the hindbrain region of the chick embryo. *Development* **113,** 1281–1291.

Neubüser, A., Peters, H., balling, R., and Martin, G. R. (1997). Antagonistic interactions between FGF and BMP signalling pathways: A mechamnism for positioning the site of tooth formation. *Cell* **90,** 247–255.

Noden, D. M. (1975). An analysis of the migratory behavior of avian cephalic neural crest cells. *Dev. Biol.* **42,** 106–130.

Ogasawara, M., Shigetani, Y., Hirano, S., Satoh, N., and Kuratani, S. (2000). *Pax1/Pax9*-related genes in an agnathan vertebrate, *Lampetra japonica:* Expression pattern of *LjPax9* implies sequential evolutionary events towards the gnathostome body plan. *Dev. Biol.* **223,** 399–410.

Osumi-Yamashita, N., Ninomiya, Y., Doi, H., and Eto, K. (1994). The contribution of both forebrain and midbrain crest cells to the mesenchyme in the frontonasal mass of mouse embryos. *Dev. Biol.* **164,** 409–419.

Sechrist, J., Scherson, T., and Bronner-Fraser, M. (1994). Rhombomere rotation reveals that multiple mechanisms contribute to the segmental pattern of hindbrain neural crest migration. *Development* **120,** 1777–1790.

Shigetani, Y., Aizawa, S., and Kuratani, S. (1995). Overlapping origins of pharyngeal arch crest cells on the postotic hindbrain. *Dev. Growth Differ.* **37,** 733–746.

Thesleff, I., Vaahtokari, A., and Partanen, A. M. (1995). Regulation of organogenesis: Common molecular mechanisms regulating the development of teeth and other organs. *Int. J. Dev. Biol.* **39,** 35–50.

Thomas, B. L., Liu, J. K., Rubenstein, J. L. R., and Sharpe, P. T. (2000). Independent regulaion of *Dlx2* expression in the epithelium and mesenchyme of the first branchial arch. *Development* **127,** 217–224.

Trumpp, A., Depew, M. J., Rubenstein, J. L. R., Bishop, J. M., and Martin, G. R. (1999). Cre-mediated gene inactivation demonstrates that FGF8 is reuired for cell survival and patterning of the first branchial arch. *Genes Dev.* **13,** 3136–3148.

Tucker, A. S., Al Khaims, A., and Sharpe, P. T. (1998a). Interactions between *Bmp-4* and *Msx-1* act to restrict gene expression to odontogenic mesenchyme. *Dev. Dyn.* **212,** 533–539.

Tucker, A. S., Matthews, K. L., and Sharpe, P. T. (1998b). Transformation of tooth type induced by inhibition of Bmp signalling. *Science* **282,** 1136–1138.

Tucker, A. S., Yamada, G., Grigoriou, M., Pachnis, V., and Sharpe, P. T. (1999a). Fgf-8 determines rostral–caudal polarity in the first branchial arch. *Development* **126,** 51–61.

Tucker, A. S., Khamis, A. A., Ferguson, C. A., Bach, I., Rosenfeld, M. G., and Sharpe, P. T. (1999b). Conserved regulation of mesenchymal gene expression by *Fgf-8* in face and limb development. *Development* **126,** 221–228.

Received for publication March 10, 2000
Revised September 6, 2000
Accepted September 7, 2000
Published online November 2, 2000